Applied Surface Science 671 (2024) 160659

Contents lists available at ScienceDirect

Applied Surface Science

journal homepage: www.elsevier.com/locate/apsusc

Full Length Article

Revisiting greenhouse gases adsorption in carbon nanostructures: Advances through a combined first-principles and molecular simulation approach

Henrique M. Cezar [a,b,*], Teresa D. Lanna [a], Daniela A. Damasceno [a,c], Alexsandro Kirch [a,c], Caetano R. Miranda [a,*]

[a] Universidade de Sao Paulo, Instituto de Fisica, Rua do Matao 1371, Sao Paulo, SP 05508-090, Brazil
[b] Hylleraas Centre for Quantum Molecular Sciences and Department of Chemistry, University of Oslo, PO Box 1033 Blindern, 0315 Oslo, Norway
[c] Department of Mechatronics and Mechanical Systems Engineering, Polytechnic School of the University of São Paulo, São Paulo 05508-030, SP, Brazil

ARTICLE INFO

Keywords:
Force field parametrization
Graphene-like structures
Carbon nanotubes
Confinement Effects
Carbon dioxide
Methane

ABSTRACT

Carbon nanostructures are promising materials to improve the performance of current gas separation membrane technologies. From the molecular modeling perspective, an accurate description of the interfacial interactions is mandatory to understand the gas selectivity in the context of greenhouse gases applications. Most of the molecular dynamics simulations studies considered available force fields with the standard Lorentz-Berthelot (LB) mixing rules to describe the interaction among carbon dioxide (CO_2), methane (CH_4) and carbon structures. We performed a systematic study in which we showed the LB underestimates the interaction energies compared to the density functional theory (DFT) results. To improve the classical description, we propose a new parametrization for the cross-terms of the Lenard-Jones potential by fitting DFT forces and energies. The effects of the new parametrization on the gases adsorption within single-walled carbon nanotubes (SWCNTs), are investigated with Grand Canonical Monte Carlo simulations. We observed considerable differences in the CO_2 and CH_4 density within SWCNTs compared to those obtained with the standard approach. Our study highlights the importance of going beyond the traditional LB mixing rules in studies involving solid/fluid interfaces of confined systems. The revised mixing terms enhanced fluid/carbon interface description with excellent transferability ranging from SWCNTs to graphene.

1. Introduction

The increasing interest in developing innovative technologies and processes for carbon capture and storage has driven several studies toward breakthroughs involving methane (CH_4) and carbon dioxide (CO_2) confined within carbon nanotubes (CNTs) [1]. CNTs emerged as a promising material for developing of new gas separation devices [2] due to their adsorption capability [3], fast mass transport [4], and mechanical strength [5,6].

Single-walled carbon nanotubes (SWCNTs) have been used as a host of a large variety of guest fillers, such as water [7], CO_2 [8], CH_4 [9], and hydrogen [10]. Computational molecular modeling is thus an essential tool for understanding underlying molecular mechanisms in chemical and physical processes of confined systems, providing atomic-level information that is often not accessible through experiments. However, the prediction success of these studies relies on using suitable force fields that provide an accurate description of the nanoscopic materials.

Previous studies also addressed the issue of CO_2 and CH_4 adsorption in graphene [11–13] and SWCNTs [14–16] within the density functional (DFT) approach. Other studies discussed how the available DFT exchange and correlation functionals describe these systems [12,13]. Using molecular dynamics (MD) and grand canonical Monte Carlo (GCMC) simulations, the adsorption of CO_2 and CH_4 molecules in carbon structures have been widely studied with a variety of force fields for both nanotube and gas molecules [8,9,17–20].

For molecular simulations, many complex and accurate force fields may be used, usually with complexity bringing extra computational cost, which may limit the simulation length and system sizes. Here, we stick to models based on Lennard-Jones interactions. In such cases, previous MD and GCMC studies considered the Lorentz-Berthelot (LB) mixing rules for the cross parameters. For CO_2, it has been shown that different three-site models provide similar densities inside the CNT when the same potential is used for the SWCNTs [8]. The reason is that the Lennard-Jones parameters of these molecular models are usually

* Corresponding authors at: Universidade de Sao Paulo, Instituto de Fisica, Rua do Matao 1371, Sao Paulo, SP 05508-090, Brazil.
E-mail addresses: h.m.cezar@kjemi.uio.no (H.M. Cezar), crmiranda@usp.br (C.R. Miranda).

https://doi.org/10.1016/j.apsusc.2024.160659
Received 16 May 2024; Received in revised form 26 June 2024; Accepted 4 July 2024
Available online 14 July 2024

similar. However, the available Lennard-Jones parameters for the SWCNTs may differ considerably, with energy potential well depths varying by almost 100 %.

Employing the Steele potential [21] with LB mixing rules is a common approach in describing fluid/graphene-like interfaces [9,22–30]. Other studies [18,20,31] employed the same mixing rules but considered different CNT potentials, such as the AMBER96 [8,19]. These studies have not provided strong arguments towards the preference for a specific force field, nor have they compared the potentials with first-principles data or discussed their influence on the adsorption properties and fluid density, for instance.

The current work systematically compares several of the most popular existing force fields and provides optimized nonbonded cross parameters to describe CO_2–SWCNTs and CH_4–SWCNTs interfaces. These parameters were obtained by fitting interaction energies and forces from DFT calculations. The parameterization was tested in configurations out of the fitting set, displaying results very similar to the ones obtained with the DFT approach. Using GCMC simulations, we showed that the standard approach using the LB mixing rules underestimates the gas density inside the SWCNT, while our potential overcomes this limitation. Thus showing the importance of going beyond the traditional LB mixing rules for confined systems in the context of greenhouse gases adsorption in carbon nanostructures.

2. Methodology

2.1. DFT

Density functional theory (DFT) calculations were performed with the Siesta [32] package considering norm-conserving pseudopotentials, localized atomic orbitals with a double-zeta polarized (DZP) basis set, and 400 Ry mesh cutoff. Structure relaxations were performed considering the convergence criteria for the forces smaller than 10^{-4} eV/Å. Besides the standard local density functional (LDA) [33], three of the most popular exchange and correlation functionals that include van der Waals corrections (vdW-DFs) were employed in our calculations, namely, the functional by Klimes, Bowler, and Michaelides (KBM or optB86b-vdW) [34], the exchange–correlation potential parameterized by Cooper, known as C09 functional [35], and the BH exchange functional by Kristian Berland and Per Hyldgaard [36] (access the Supporting Information (SI) section S1 to see a brief description of these functionals).

The graphene sheet was modeled with a 2 × 2 × 1 supercell with 30 Å vacuum to allow a similar molecular coverage compared to the experimental reference data [12]. We also considered a 5 × 5 × 1 supercell configuration to exclude the interactions between neighboring molecules. For these calculations, we used a mesh equivalently to 16 × 16 × 1 k-points per unit cell within the Monkhorst-pack scheme to sample the Brillouin zone. Besides the graphene sheets, we performed a similar study on (8,8), (10,10) and (0,17) SWCNTs with 20 Å length to explore chirality and diameter effects.

2.2. Force fields

Interaction energies were evaluated with the LAMMPS package [37] considering the implementation of non-bonded contribution within the classical force field given by:

$$U_{inter} = \sum_{i<j} 4\epsilon_{ij}\left[\left(\frac{\sigma_{ij}}{r_{ij}}\right)^{12} - \left(\frac{\sigma_{ij}}{r_{ij}}\right)^{6}\right] + \sum_{i<j}\frac{q_i q_j}{r_{ij}}, \quad (1)$$

where ϵ_{ij}, σ_{ij} are the Lennard-Jones parameters, $q_{i(j)}$ the atomic charge, and r_{ij} is the separation distance. The molecules and carbon structures were kept rigid during the simulations.

We considered six different sets of Lennard-Jones parameters for the graphene/CNT system, taken from AIREBO [38], Mao [39], Huang [18], AMBER96 [40], Walther [41], and Steele [21] force fields, all previously employed in adsorption studies. For CH_4, we considered the OPLS-AA [42] potential, while CO_2 was modeled using the EPM2 [43] model, these being among the most popular and accurate force fields found in the literature. All the parameters are given in Table S1 in SI. For these force fields, cross terms describing the interaction between atomic species were obtained with the Lorentz-Berthelot mixing rules, i.e., $\epsilon_{ij} = \sqrt{\epsilon_{ii}\epsilon_{jj}}$ and $\sigma_{ij} = (\sigma_{ii} + \sigma_{jj})/2$, as it was used in several works found in the literature [9,22–30].

Graphene-like structures potentially have three adsorption sites, i.e., top (T), bridge (B), and hollow (H), as depicted in Fig. 1a. Among the possibilities, some typical and stable molecular orientations besides these sites (see Fig. 1a–g) were considered in our calculations to evaluate the interaction energy curves and forces with both DFT and classical FFs. Within these approaches, the interaction energy, E_{int}, is given by

$$E_{int} = E_{tot} - [E_{Car} + E_{Mol}], \quad (2)$$

where E_{tot} is the system's total energy; E_{Car} and E_{Mol} are the energies of the isolated carbon material (CNT or graphene) and the adsorbed molecule, respectively.

2.3. Parametrization process

We obtained a new set of Lennard-Jones cross parameters optimized for the CO_2-SWCNT and CH_4-SWCNT interfaces using the DFT interaction energies and atomic forces. We considered only the mixing terms between the gas and carbon nanostructure, keeping all other parameters intact. The data was fitted with the GULP package [44]. To obtain a better fit around the minimum of the energy curve, and provide a better description of the equilibrium distances, we weighted (w) the configurations according to the equation:

$$w = exp[(E_{int} - E_{int}^{min})/kT], \quad (3)$$

where E_{int}^{min} is the minimum energy point among the curves used in the fitting process and temperature T was defined as 200 K and 300 K for CH_4 and CO_2, respectively. These values were selected to obtain a good balance between the description of the interaction energy minimum and over the entire curve. The weight for the interaction energy was multiplied by 10^3 to get similar contributions as for the forces. This procedure is necessary because there are $3N$ (with $N \approx 350$ being the number of atoms in each calculation) force components for each interaction energy point; therefore, the 10^3 factor evens the contribution between the forces and energy during the fitting.

2.4. GCMC

To evaluate the impact of the force fields on the adsorption of the gases within SWCNTs, we performed GCMC simulations using the Cassandra package [45]. With this approach, first the chemical potentials of both CO_2 and CH_4 at 300 K and 1 atm were obtained using the Widom insertion method [46]. These simulations were performed in the *NPT* ensemble with 1×10^6 followed by 3×10^6 steps in thermalization and production phases, respectively.

Subsequently, the SWCNTs with 200 Å lengths were loaded with up to 200 gas molecules, depending on their diameter. An *NVT* simulation was run for 5×10^4 steps to generate the initial configuration. This process was followed by the GCMC using insertions restricted by the SWCNTs cylinder geometry. These simulations were performed for 5×10^6 steps, using configurational-biased insertions (with 16 trial insertions) and considering probabilities of 25 % for each of the translation, rotation, insertion, and deletion moves. The simulations were long enough to reach the convergence of both internal energy and the number of adsorbed molecules.

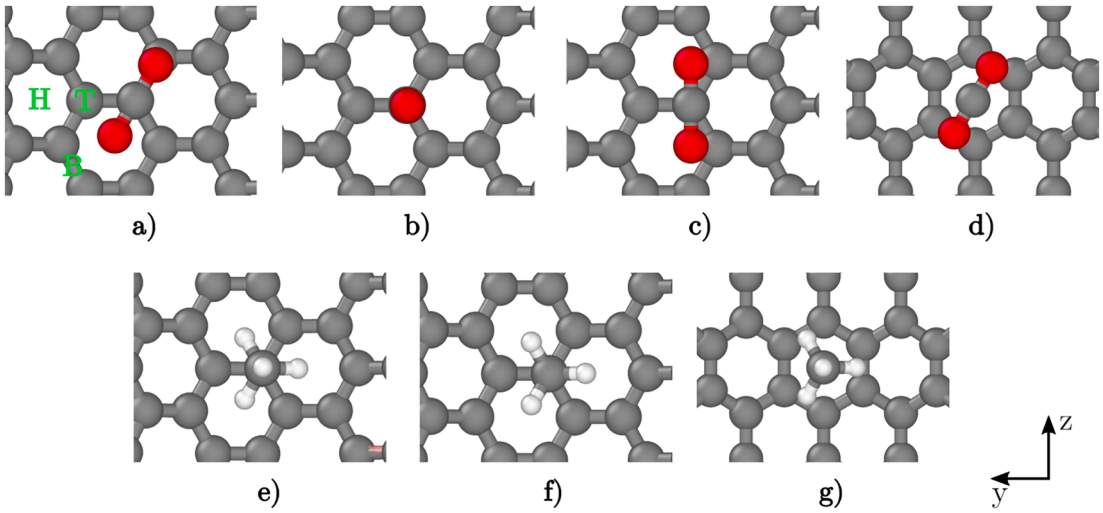

Fig. 1. Some common and stable molecular configurations on the carbon structures's adsorption sites for both CO_2 a-d and CH_4 e-g considered in our calculations. Colors: Gray (carbon), red (oxygen), white (hydrogen). Fig. 1a also exhibits the typical adsorption sites – hollow (H), top (T), bridge (B) – in graphene-like lattices.

3. Results and discussions

3.1. DFT functional

We benchmarked the DFT functionals against experimental data to establish the most appropriate functional to describe the interaction between CO_2 and CH_4 molecules and the graphene monolayer. The interaction energy curves obtained by applying Equation 2 as a function of distance r from the $2 \times 2 \times 1$ graphene sheet are shown in Fig. 2a (CO_2) and Fig. 2b (CH_4). Comparing these curves for CO_2, BH gives a slight deviation from C09 and KBM functional. The equilibrium distance and energy predicted by BH are 3.20 Å and −5.83 kcal/mol, respectively. These values for the C09 are 3.11 Å and −6.44 kcal/mol; while the KBM gave 3.12 Å and −6.44 kcal/mol. Our results for the C09 and KBM are in good agreement with the experimental results reported in the literature (-6.26 kcal/mol) under similar conditions [12]. LDA displayed a significant deviation despite the equilibrium distance being in good agreement with C09 and KBM, showing the importance of considering the long-range contributions in the DFT calculations.

Osouleddini et al. [11], using the hybrid X3LYP functional, reported the CO_2-graphene adsorption energy and equilibrium distance as being −0.69 kcal/mol and 3.12 Å, respectively. In turn, Takeuchi et al. [12] using vdW-DF1, optB86b-vdW (KBM), and rev-vdW-DF2, found E_{int} equal to −5.80, −5.90 and −4.08 kcal/mol, respectively. They also reported the equilibrium distance for the vdW-DF1 and optB86b-vdW as being 3.4 Å and 3.2 Å, respectively. The minor differences observed in their KBM result in comparison to ours may be attributed to the use of different geometries, software, and a distinct basis set. Other E_{int} values reported in the literature range from −4.11 to −5.99 kcal/mol [47].

The CH_4-graphene interaction energy curves display a similar pattern observed for the CO_2 case, (see Fig. 2b). For the BH functional, the obtained equilibrium distance and minimum interaction energy were 3.39 Å and −4.55 kcal/mol, respectively. For C09, these values are 3.26 Å and −5.09 kcal/mol, and for KBM, 3.28 Å and −5.15 kcal/mol. For the same configuration, Thierfelder et al. [13] found the equilibrium distance ranging from 3.05 to 3.99 Å and minimum interaction energy varying from −0.23 to −7.38 kcal/mol, using several DFT functional flavors and second order Møller–Plesset perturbation theory. In contrast, Osouleddini et al. [11] found a similar equilibrium distance of 3.35 Å, but lower adsorption energy of −1.15 kcal/mol.

Most of the experimental results are available for the methane-graphite whereby the equilibrium distance and desorption energy ranges from 3.21 to 4.27 Å and 2.73 to 4.6 kcal/mol, respectively [48]. In the absence of accurate experimental results for similar coverage of the CH_4-graphene system, such as the ones available for CO_2 [12], we argue that any of the studied van der Waals functionals can describe the interfaces accurately enough for the fitting with Lennard-Jones parameters, since our results are in the same range as the values reported in the literature for the methane-graphite interface.

There are no strong arguments towards selecting either C09 or KBM, as both give very similar results, compatible with the experimental desorption energies for CO_2. As an advantage, the KBM functional has been implemented so far in more *ab initio* software than C09. Comparing C09 and KBM implementations in Siesta, the KBM performed more

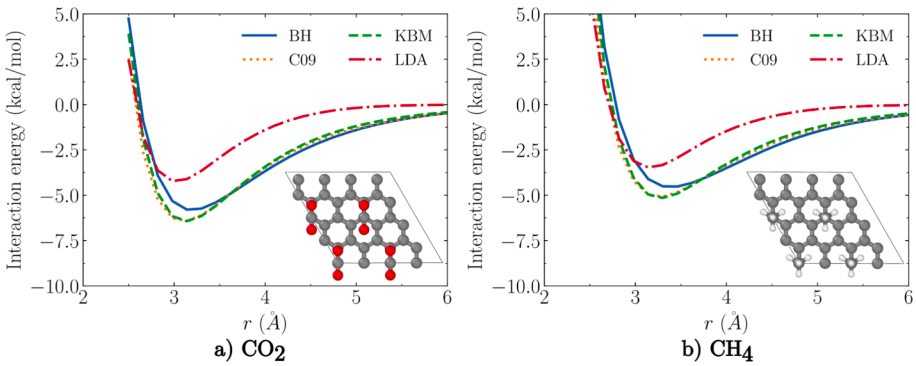

Fig. 2. The interaction energy curves of CO_2-graphene (a) and CH_4-graphene (b) (2x2x1 supercell) interface using the LDA, BH, KBM, and C09 functionals. For this study, we considered the most energetically favored adsorption configuration represented in Fig. 1a and Fig. 1e, for CO_2 and CH_4, respectively.

efficiently than C09 for our systems. For these reasons, we chose the KBM functional to extract the new set of Lennard-Jones cross parameters optimized for the CO_2-SWCNT and CH_4-SWCNT description for consistency.

3.2. FF parametrization

We evaluated the performance of the selected classical FFs using the Lorentz-Berthelot mixing rules in describing the CO_2-SWCNT and CH_4-SWCNT interfaces, by comparing the corresponding interaction energy curves with the DFT results (see section S3 for more details). For the investigated adsorption configurations, all FFs curves exhibited a smaller depth than the DFT-KBM functional (see Fig. 3 a,b). Also, the equilibrium distance is slightly smaller, with the Walther potential displaying the greatest discrepancy. These differences can lead to an inadequate description of the gas adsorption on the carbon structures.

The inconsistency observed between classical FFs and DFT calculations suggests the need for a more refined parametrization. By using our approach to fit the Lennard-Jones cross parameters, ϵ_{ij} and σ_{ij}, to the DFT-KBM dataset, we obtained the optimized parameters shown in Table 1. These parameters were obtained considering different adsorption sites and carbon nanostructures, aiming at the transferability and accurate description of energy and forces during simulations. More details about the dataset are given in section S3.

The energy curve with the optimized parameters agrees with the DFT results and improves the forces, potential well depth, and equilibrium distances concerning the standard approach. The quality of our fit can be illustrated by the correlation between the classical and DFT-KBM interaction energies. We obtained a Pearson correlation coefficient for the fitted and DFT interaction energies of 0.953 and 0.974 for CO_2 and CH_4, respectively. The forces' correlations are smaller, having coefficients of up to 0.699 and 0.659 for CO_2 and CH_4, respectively. Figures showing the correlations and further discussion are presented in section S4.

Fig. 3 a,b) illustrates the comparison between the interaction energies computed with the FFs, our parameterized cross terms, and the DFT-KBM models. We highlight that one of the most used FFs for describing adsorption in such systems, Steele's FF, shows the smallest E_{int}, in disagreement with the DFT data. Our fitted parameters also improve the energy difference at the center of the nanotube and the minimum. This value is important for adsorption studies as it is what is effectively seen by the Monte Carlo simulations.

We tested the obtained parameterization in different configurations not present in the fitting set (see Fig. 4a–d and section S3 of SI). By considering distinguished systems, we evaluated the transferability of the LJ parameters to other chemical environments. In these new systems, the fitted curve showed a remarkable agreement with KBM results, even though these configurations were not considered in the fitting process.

In all the cases, our fitted model improved the adsorption energy description with respect to the existing FFs combined with the traditional Lorentz-Berthelot mixing rules, confirming the parametrization accuracy in describing fluid-carbon interfaces. Also, the fitted and KBM curves agreed well with the energy depth and equilibrium distance for both a smaller radius SWCNT and the infinite limit (graphene), showing their remarkable transferability capability.

Table 1
Crossing terms for the LJ potential optimized by the fitting process.

	ϵ_{ij}(K)	σ_{ij}(\AA)
C_{CNT}-C_{CO2}	74.466	3.09
C_{CNT}-O_{CO2}	85.189	3.09
C_{CNT}-C_{CH4}	66.540	3.38
C_{CNT}-H_{CH4}	49.609	2.57

3.3. Gas adsorption in the SWCNTs

The discrepancy observed between classical FFs employing Lorentz-Berthelot mixing rules and the DFT calculations indicates that the structuring and distribution of gas molecules inside the SWCNTs may also differ. In this context, we compared the densities obtained with existing classical FFs with the ones using the optimized LJ cross parameters as a function of the tube diameter. Fig. 5a,b show the gas densities obtained with GCMC for the (6,6), (12,12) and (16,16) SWCNTs.

The fluid density within the CNTs strongly depends on the adopted force field and tube diameter. For the CO_2 case, we observed the AIREBO and Steele curves give a consistent decrease in fluid density as the nanotube diameter increases (see Fig. 5a). Regarding the other FFs, the density increases as the nanotube increases from 8.1 Å (6,6) to 16.3 Å (12,12), and decreases as the nanotube increases from 16.3 Å (12,12) to 21.7 Å (16,16). A similar trend was observed by Alexiadis and Kassinos [8] using MD. Also, the amount of CO_2 in the nanotubes predicted by the traditional classical FFs is much lower than that obtained with our fitted model. The densities obtained within the Steele potential and LB mixing rules can be up to seven times smaller than the ones predicted by our fitted potential for the (16,16) SWCNT.

For the CH_4 case (Fig. 5b), density curves obtained with AIREBO, Mao, Huang, AMBER, and Steele curves display a similar trend, with the densities decreasing as the nanotube diameter increases from 8.1 Å (6,6) to 16.3 Å (12,12) and remains practically unchanged from 16.3 Å to 21.7 Å (16,16). These results differ from those obtained with the Walther potential and our fitted parameters, since the CH_4 density slightly increases as the nanotube increases from 8.1 Å to 16.3 Å and then decreases as the nanotube increases from 16.3 Å to 21.7 Å. However, the densities in the (12,12) and (16,16) are almost 50 % greater than Walther's using the fitted parameters. We reach the same conclusion as for the CO_2 case, i.e., the number of adsorbed molecules is underestimated by all the tested force fields. These results revealed the importance of revisiting the adsorption of greenhouse gases in carbon structures to approach the DFT achievements.

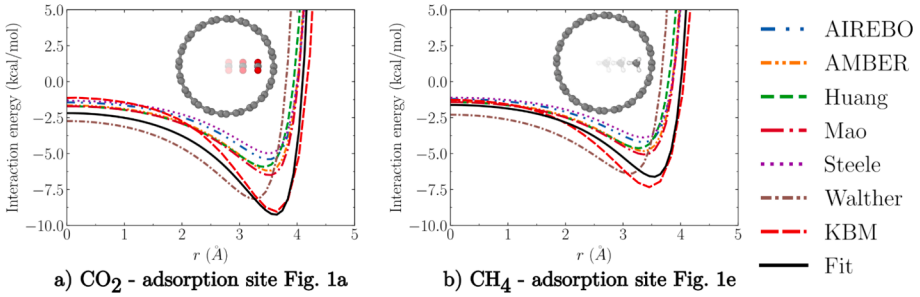

Fig. 3. The interaction energy curves of a) CO_2 and b) CH_4 adsorbed on the (10,10) SWCNT. Here we compare the classical FFs performance against the DFT (KBM), and the parameterized potential (Fit).

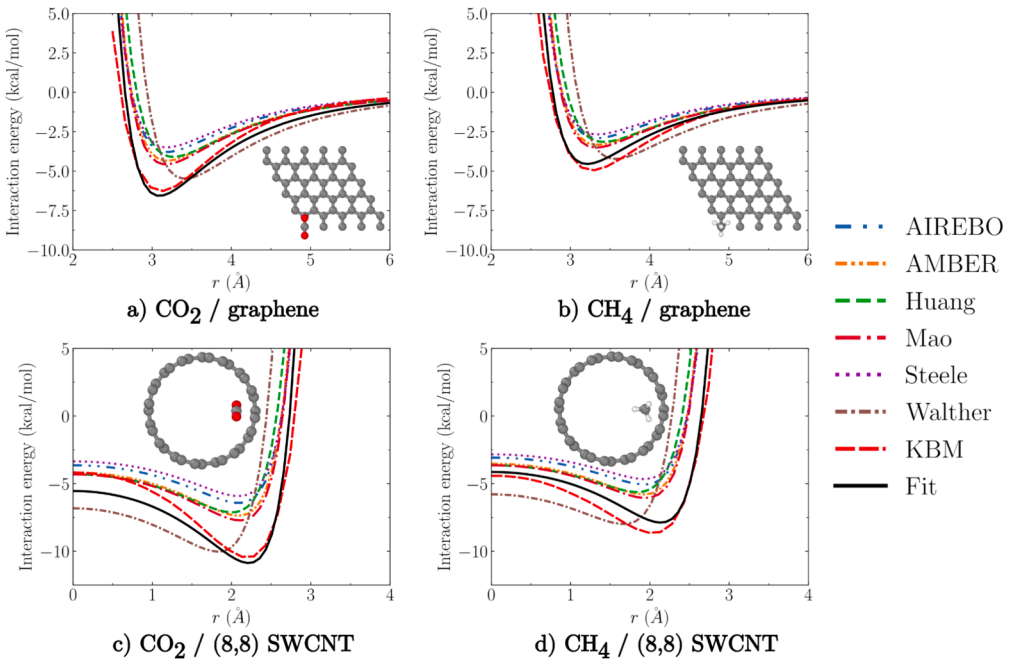

Fig. 4. The interaction energy curves of a) CO_2 and b) CH_4 above the graphene sheet and c) CO_2 and d) CH_4 adsorbed in an (8,8) SWCNT. These systems were apart from the fitting set configurations, therefore, showing how the fitted parameters perform for interactions beyond the fitted situations.

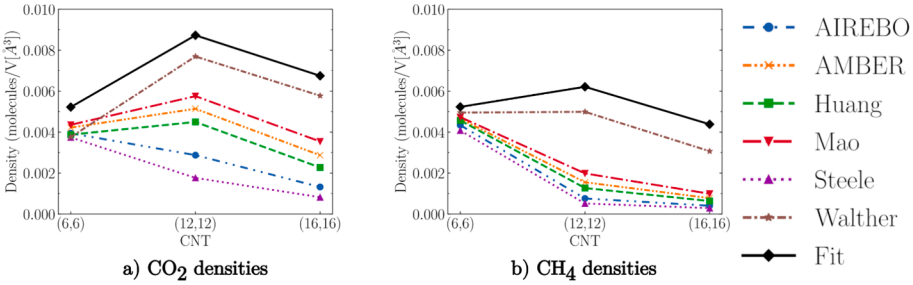

Fig. 5. Comparison of the density of a) CO_2 and b) CH_4 in (6,6), (12,12) and (16,16) CNTs.

4. Conclusions

The differences observed in the performance of DFT functionals and classical FFs in describing the adsorption of CH_4 and CO_2 in carbon structures have been addressed in our investigation. We proposed a new set of LJ cross parameters obtained by fitting DFT energies and forces. The accuracy in estimating the adsorption properties has been established by a systematic comparison with DFT results.

Among the DFT functionals considered in our study, the KBM flavor could properly describe the adsorption of CO_2 and CH_4 in carbon structures in accordance with previous experimental studies. Considering different adsorption sites and nanotube chirality, we have fitted a new set of Lennard-Jones cross parameters ϵ_{ij} and σ_{ij}. These parameters enhanced the fluid/solid interface description considerably with respect to the existing FFs, which use the standard Lorentz-Berthelot mixing rules. Most FFs underestimate the adsorption energy and equilibrium distances. Regarding the adsorption energies, the Walther potential has a deeper well if compared with the other FFs, but it is closer to the reference DFT calculations, being about 20 % shallower. These differences with respect to the DFT results can be up to 100 % for the other FFs, including the popular Steele and AMBER potentials.

The fitted model was employed beyond the fitting set, and it showed great transferability capability. Furthermore, using GCMC, we investigated the adsorption features of CO_2 and CH_4 in SWCNTs of different sizes. Our GCMC simulations showed that the standard approach using the Lorentz-Berthelot mixing rules underestimates the gas density inside the SWCNT. Our parameters are only for the interface mixing interactions, and can be used with any set of LJ-based force fields for the gases and carbon nanostructures.

These results highlight the importance of going beyond the Lorentz-Berthelot mixing rules involving fluid/carbon interfaces. The procedure employed in this work may be used for the parametrization of functional groups such as carboxyl or hydroxyl, often present in carbon nanostructure defects. We highlight that our findings may improve the molecular modeling studies involving challenging problems within the carbon dioxide capture, utilization and storage context.

CRediT authorship contribution statement

Henrique M. Cezar: Conceptualization, Formal analysis, Investigation (classical simulations), Software, Visualization. **Teresa D. Lanna:** Methodology, Software, Formal analysis, Investigation (DFT), Visualization. **Daniela A. Damasceno:** Conceptualization, Writing – original draft. **Alexsandro Kirch:** Formal analysis, Writing – review & editing. **Caetano R. Miranda:** Conceptualization, Resources, Writing – review & editing, Supervision, Funding acquisition.

Declaration of competing interest

The authors declare that they have no known competing financial

interests or personal relationships that could have appeared to influence the work reported in this paper.

Data availability

Data will be made available on request.

Acknowledgements

We gratefully acknowledge support of the RCGI – Research Centre for Gas Innovation, hosted by the University of São Paulo (USP) and sponsored by FAPESP – São Paulo Research Foundation (2014/50279-4 and 2020/15230-5) and Shell Brasil, and the strategic importance of the support given by ANP (Brazil's National Oil, Natural Gas and Biofuels Agency) through the R&D levy regulation. We also thank the financial support of FAPESP through project numbers #2017/02317-2, #2019/21430-0, and #2020/01558-9, and the National Council for Scientific and Technological Development (CNPq) through grant 307064/2019-0 for financial support. HMC also thanks the Research Council of Norway through the Centre of Excellence Hylleraas Centre for Quantum Molecular Sciences (grant number 262695). The computational time for the calculations was provided by High-Performance Computing facilities at the University of São Paulo (USP). We thank Julian D. Gale for the insightful discussions regarding the parametrization using GULP.

Appendix A. Supplementary data

Supplementary data to this article can be found online at https://doi.org/10.1016/j.apsusc.2024.160659.

References

[1] Y.R. Poudel, W. Li, Synthesis, properties, and applications of carbon nanotubes filled with foreign materials: a review, Mater. Today Phys. 7 (2018) 7–34.
[2] B. Van der Bruggen, The separation power of nanotubes in membranes: A review, ISRN Nanotechnol. 2012 (2012) 1–17.
[3] M. Calvaresi, F. Zerbetto, Atomistic molecular dynamics simulations reveal insights into adsorption, packing, and fluxes of molecules with carbon nanotubes, J. Mater. Chem. A Mater. Energy Sustain. 2 (2014) 12123–12135.
[4] J.K. Holt, H.G. Park, Y. Wang, M. Stadermann, A.B. Artyukhin, C.P. Grigoropoulos, A. Noy, O. Bakajin, Fast mass transport through sub-2-nanometer carbon nanotubes, Science. 312 (2006) 1034–1037.
[5] C.-C. Chang, I.-K. Hsu, M. Aykol, W.-H. Hung, C.-C. Chen, S.B. Cronin, A new lower limit for the ultimate breaking strain of carbon nanotubes, ACS Nano. 4 (2010) 5095–5100.
[6] R. Zhang, Q. Wen, W. Qian, D.S. Su, Q. Zhang, F. Wei, Superstrong ultralong carbon nanotubes for mechanical energy storage, Adv. Mater. 23 (2011) 3387–3391.
[7] G. Hummer, J.C. Rasaiah, J.P. Noworyta, Water conduction through the hydrophobic channel of a carbon nanotube, Nature. 414 (2001) 188–190.
[8] A. Alexiadis, S. Kassinos, Molecular dynamic simulations of carbon nanotubes in CO2 atmosphere, Chem. Phys. Lett. 460 (2008) 512–516.
[9] G.P. Lithoxoos, A. Labropoulos, L.D. Peristeras, N. Kanellopoulos, J. Samios, I. G. Economou, Adsorption of N2, CH4, CO and CO2 gases in single walled carbon nanotubes: A combined experimental and Monte Carlo molecular simulation study, J. Supercrit. Fluids. 55 (2010) 510–523.
[10] A.C. Dillon, K.M. Jones, T.A. Bekkedahl, C.H. Kiang, D.S. Bethune, M.J. Heben, Storage of hydrogen in single-walled carbon nanotubes, Nature. 386 (1997) 377–379.
[11] N. Osouleddini, S.F. Rastegar, DFT study of the CO2 and CH4 assisted adsorption on the surface of graphene, J. Electron Spectros. Relat. Phenomena. 232 (2018) 105–110.
[12] K. Takeuchi, S. Yamamoto, Y. Hamamoto, Y. Shiozawa, K. Tashima, H. Fukidome, T. Koitaya, K. Mukai, S. Yoshimoto, M. Suemitsu, Y. Morikawa, J. Yoshinobu, I. Matsuda, Adsorption of CO2 on graphene: A combined TPD, XPS, and vdW-DF study, J. Phys. Chem. C Nanomater. Interfaces. 121 (2017) 2807–2814.
[13] C. Thierfelder, M. Witte, S. Blankenburg, E. Rauls, W.G. Schmidt, Methane adsorption on graphene from first principles including dispersion interaction, Surf. Sci. 605 (2011) 746–749.
[14] M.D. Ganji, M. Asghary, A.A. Najafi, Interaction of methane with single-walled carbon nanotubes: Role of defects, curvature and nanotubes type, Commun. Theor. Phys. 53 (2010) 987–993.
[15] D. Quiñonero, A. Frontera, P.M. Deyà, Feasibility of single-walled carbon nanotubes as materials for CO2 adsorption: A DFT study, J. Phys. Chem. C Nanomater. Interfaces. 116 (2012) 21083–21092.
[16] J. Zhao, A. Buldum, J. Han, J.P. Lu, Gas molecule adsorption in carbon nanotubes and nanotube bundles, Nanotechnology. 13 (2002) 195–200.
[17] T. Düren, F.J. Keil, Molecular Modeling of Adsorption in Carbon Nanotubes, Chemical Engineering & Technology. 24 (2001) 698–702, https://doi.org/10.1002/1521-4125(200107)24:7<698::aid-ceat698>3.0.co;2-m.
[18] L. Huang, L. Zhang, Q. Shao, L. Lu, X. Lu, S. Jiang, W. Shen, Simulations of binary mixture adsorption of carbon dioxide and methane in carbon nanotubes: Temperature, pressure, and pore size effects, J. Phys. Chem. C Nanomater. Interfaces. 111 (2007) 11912–11920.
[19] M. Rahimi, J.K. Singh, D.J. Babu, J.J. Schneider, F. Müller-Plathe, Understanding carbon dioxide adsorption in carbon nanotube arrays: Molecular simulation and adsorption measurements, J. Phys. Chem. C Nanomater. Interfaces. 117 (2013) 13492–13501.
[20] S. Wang, L. Lu, X. Lu, W. Cao, Y. Zhu, Adsorption of binary CO2/CH4mixtures using carbon nanotubes: Effects of confinement and surface functionalization, Sep. Sci. Technol. 51 (2016) 1079–1092.
[21] W.A. Steele, The interaction of rare gas atoms with graphitized carbon black, J. Phys. Chem. 82 (1978) 817–821.
[22] R.F. Cracknell, D. Nicholson, K.E. Gubbins, Molecular dynamics study of the self-diffusion of supercritical methane in slit-shaped graphitic micropores, J. Chem. Soc. Faraday Trans. 91 (1995) 1377.
[23] A.I. Skoulidas, D.S. Sholl, J.K. Johnson, Adsorption and diffusion of carbon dioxide and nitrogen through single-walled carbon nanotube membranes, J. Chem. Phys. 124 (2006) 054708.
[24] E.J. Bottani, V. Bakaev, W. Steele, A simulation/experimental study of the thermodynamic properties of carbon dioxide on graphite, Chem. Eng. Sci. 49 (1994) 2931–2939.
[25] K. Bartuś, A. Bródka, Temperature study of structure and dynamics of methane in carbon nanotubes, J. Phys. Chem. C Nanomater. Interfaces. 118 (2014) 12010–12016.
[26] K. Bartuś, A. Bródka, Methane behavior in carbon nanotube as a function of pore filling and temperature studied by molecular dynamics simulations, J. Phys. Chem. C Nanomater. Interfaces. 121 (2017) 4066–4073.
[27] K. Bartuś, A. Bródka, Methane in carbon nanotube: molecular dynamics simulation, Mol. Phys. 109 (2011) 1691–1699.
[28] L. Liu, D. Nicholson, S.K. Bhatia, Adsorption of CH4 and CH4/CO2 mixtures in carbon nanotubes and disordered carbons: A molecular simulation study, Chem. Eng. Sci. 121 (2015) 268–278.
[29] P. Kowalczyk, S. Furmaniak, P.A. Gauden, A.P. Terzyk, Optimal single-walled carbon nanotube vessels for short-term reversible storage of carbon dioxide at ambient temperatures, J. Phys. Chem. C Nanomater. Interfaces. 114 (2010) 21465–21473.
[30] A. Vishnyakov, P.I. Ravikovitch, A.V. Neimark, Molecular level models for CO2Sorption in nanopores, Langmuir. 15 (1999) 8736–8742.
[31] W. Cao, L. Lu, M. Zhou, G.M. Tow, L. Huang, T. Yang, X. Lu, Hydrophilicity effect on CO2/CH4 separation using carbon nanotube membranes: insights from molecular simulation, Mol. Simul. 43 (2017) 502–509.
[32] J.M. Soler, E. Artacho, J.D. Gale, A. García, J. Junquera, P. Ordejón, D. Sánchez-Portal, The SIESTA method forab initioorder-Nmaterials simulation, J. Phys. Condens. Matter. 14 (2002) 2745–2779.
[33] D.M. Ceperley, B.J. Alder, Ground state of the electron gas by a stochastic method, Phys. Rev. Lett. 45 (1980) 566–569.
[34] J. Klimeš, D.R. Bowler, A. Michaelides, Van der Waals density functionals applied to solids, Phys. Rev. B Condens. Matter Mater. Phys. 83 (2011), https://doi.org/10.1103/physrevb.83.195131.
[35] V.R. Cooper, Van der Waals density functional: An appropriate exchange functional, Phys. Rev. B Condens. Matter Mater. Phys. 81 (2010), https://doi.org/10.1103/physrevb.81.161104.
[36] K. Berland, P. Hyldgaard, Exchange functional that tests the robustness of the plasmon description of the van der Waals density functional, Phys. Rev. B Condens. Matter Mater. Phys. 89 (2014), https://doi.org/10.1103/physrevb.89.035412.
[37] S. Plimpton, Fast parallel algorithms for short-range molecular dynamics, J. Comput. Phys. 117 (1995) 1–19.
[38] D.W. Brenner, O.A. Shenderova, J.A. Harrison, S.J. Stuart, B. Ni, S.B. Sinnott, A second-generation reactive empirical bond order (REBO) potential energy expression for hydrocarbons, J. Phys. Condens. Matter. 14 (2002) 783–802.
[39] Z. Mao, A. Garg, S.B. Sinnott, Molecular dynamics simulations of the filling and decorating of carbon nanotubules, Nanotechnology. 10 (1999) 273–277.
[40] W.D. Cornell, P. Cieplak, C.I. Bayly, I.R. Gould, K.M. Merz, D.M. Ferguson, D. C. Spellmeyer, T. Fox, J.W. Caldwell, P.A. Kollman, A second generation force field for the simulation of proteins, nucleic acids, and organic molecules, J. Am. Chem. Soc. 117 (1995) 5179–5197.
[41] J.H. Walther, R. Jaffe, T. Halicioglu, P. Koumoutsakos, Carbon nanotubes in water: Structural characteristics and energetics, J. Phys. Chem. B. 105 (2001) 9980–9987.
[42] W.L. Jorgensen, D.S. Maxwell, J. Tirado-Rives, Development and testing of the OPLS all-atom force field on conformational energetics and properties of organic liquids, J. Am. Chem. Soc. 118 (1996) 11225–11236.
[43] J.G. Harris, K.H. Yung, Carbon dioxide's liquid-vapor coexistence curve and critical properties as predicted by a simple molecular model, J. Phys. Chem. 99 (1995) 12021–12024.
[44] J.D. Gale, A.L. Rohl, The General Utility Lattice Program (GULP), Molecular Simulation. 29 (2003) 291–341, https://doi.org/10.1080/0892702031000104887.
[45] J.K. Shah, E. Marin-Rimoldi, R.G. Mullen, B.P. Keene, S. Khan, A.S. Paluch, N. Rai, L.L. Romanielo, T.W. Rosch, B. Yoo, E.J. Maginn, Cassandra: An open source Monte Carlo package for molecular simulation, J. Comput. Chem. 38 (2017) 1727–1739.

[46] B. Widom, Some Topics in the Theory of Fluids, The Journal of Chemical Physics. 39 (1963) 2808–2812, https://doi.org/10.1063/1.1734110.
[47] G.M. Meconi, R. Zangi, Adsorption-induced clustering of CO on graphene, Phys. Chem. Chem. Phys. 22 (2020) 21031–21041.
[48] O.O. Adisa, B.J. Cox, J.M. Hill, Modelling the surface adsorption of methane on carbon nanostructures, Carbon N. Y. 49 (2011) 3212–3218.